Research Paper

Microinfusion Using Hollow Microneedles

Wijaya Martanto,[1] Jason S. Moore,[1] Osama Kashlan,[1] Rachna Kamath,[1] Ping M. Wang,[1] Jessica M. O'Neal,[2] and Mark R. Prausnitz[1,2,3]

Purpose. The aim of the study is to determine the effect of experimental parameters on microinfusion through hollow microneedles into skin to optimize drug delivery protocols and identify rate-limiting barriers to flow.

Methods. Glass microneedles were inserted to a depth of 720–1080 μm into human cadaver skin to microinfuse sulforhodamine solution at constant pressure. Flow rate was determined as a function of experimental parameters, such as microneedle insertion and retraction distance, infusion pressure, microneedle tip geometry, presence of hyaluronidase, and time.

Results. Single microneedles inserted into skin without retraction were able to infuse sulforhodamine solution into the skin at flow rates of 15–96 μl/h. Partial retraction of microneedles increased flow rate up to 11.6-fold. Infusion flow rate was also increased by greater insertion depth, larger infusion pressure, use of a beveled microneedle tip, and the presence of hyaluronidase such that flow rates ranging from 21 to 1130 μl/h were achieved. These effects can be explained by removing or overcoming the large flow resistance imposed by dense dermal tissue, compressed during microneedle insertion, which blocks flow from the needle tip.

Conclusions. By partially retracting microneedles after insertion and other methods to overcome flow resistance of dense dermal tissue, protocols can be designed for hollow microneedles to microinfuse fluid at therapeutically relevant rates.

KEY WORDS: hyaluronidase; infusion; MEMS; skin; transdermal drug delivery.

INTRODUCTION

Infusion pumps are used for many clinical applications, including intravenous, epidural, and subcutaneous delivery of analgesics and anesthetics, antibiotics, cardiovascular drugs, and insulin (1–5). Drug delivery via infusion reduces the plasma drug concentration fluctuation associated with oral delivery and the slow onset and long depot effect associated with transdermal patch delivery. Infusion pumps are commonly used when continuous, intermittent, or pulsatile delivery of drug is needed. They also provide an alternative for patients intolerant to oral administration and can be programmed to achieve special delivery profiles. The use of infusion pumps outside the clinical setting has been limited by the device's bulky size and expensive cost (6) as well as its low patient compliance because of the inconvenience of an indwelling catheter that has a relatively large infusion set and the expertise required to properly use it (7,8).

Recently, a compact, disposable drug delivery device that incorporates a relatively short, 5-mm-long hypodermic needle has been shown to continuously and subcutaneously infuse drug solutions, such as heparin to prevent thrombosis (9) and morphine sulfate for management of cancer pain (9,10). This type of device can be worn on the skin in a discrete and convenient manner and deliver drug from a pressure-driven reservoir through the needle into the skin. Despite its minimally invasive approach, local erythema, edema, and contact dermatitis at the injection site have been reported with the use of this type of device (11). As a further improvement, needles could be made still smaller to provide an even less invasive and painless needle to increase patient compliance.

To address this need, we and others have adapted microfabrication technology to produce needles of micron dimensions. Using technology developed by the microelectronics industry, needles measuring hundreds of microns in length can be fabricated using methods conducive to reliable, inexpensive mass production. Microneedles can be coupled with a micropump to make a wearable infusion device that is highly patient friendly and can serve as a potential replacement for conventional hypodermic needles and infusion sets. Microneedles are expected to be safe because they are minimally invasive devices that are inserted only into skin's superficial layers and are typically bloodless and painless.

[1] School of Chemical and Biomolecular Engineering and Center for Drug Design, Development and Delivery, Georgia Institute of Technology, Atlanta, Georgia 30332, USA.

[2] Wallace H. Coulter Department of Biomedical Engineering, Georgia Institute of Technology, Atlanta, Georgia 30332, USA.

[3] To whom correspondence should be addressed. (e-mail: mark.prausnitz@chbe.gatech.edu)

Microneedles are also expected to be effective as a hybrid between transdermal patches and injection/infusion.

Microneedles were originally designed to increase skin permeability for patch-based delivery by diffusion. In this application, solid microneedles have been shown to increase transdermal transport by orders of magnitude *in vitro* for a variety of compounds (12–14). *In vivo* studies have demonstrated delivery of insulin (15), oligonucleotides (16), human growth hormone (17), and desmopressin (18), as well as ovalbumin (19), DNA (20), and anthrax (21) vaccines. Human pain studies have shown that insertion of microneedles can be painless and does not cause skin irritation (20,22).

Of greater relevance to infusion, microneedles containing a hollow bore have also been made using a variety of different microfabrication approaches (23,24). Active injection using hollow microneedles coupled to a syringe or pump has been demonstrated for insulin delivery to diabetic hairless rats *in vivo* (13,25), administration of chemical stimuli into brain tissue *in vivo* (26), and injection of fluorescent dye into chicken thigh *in vitro* (27). Hollow microneedles have also been used to passively deliver insulin by diffusion to diabetic rats (28) and to extract nanoliter quantities of blood for glucose measurement in human (29).

Motivated by these studies demonstrating microinjection of drugs into skin using hollow microneedles, there is a need for systematic study of the effects of infusion parameters, and their optimization, on flow rate using hollow microneedles. Previous studies in the literature report delivery of relatively small volumes of drug solution into the skin, which were enough to have effects on rodents, but may not be sufficient to accommodate larger human doses. Previous work in our lab has shown that flow rate can be increased by changing infusion parameters, where partial retraction of the needle after deeper insertion was especially beneficial (30). To address the need to increase and control infusion rate, this study sought to experimentally quantify the relationship between infusion flow rate and different experimental parameters, such as needle insertion depth, retraction distance, infusion pressure, needle geometry, and the presence of hyaluronidase. We therefore used single glass microneedles to infuse sulforhodamine solution into human cadaver skin and measured the infusion flow rate as a function of various experimental parameters. The resulting data were used to determine optimal infusion protocols and identify rate-limiting barriers to flow. Analysis was guided by the hypothesis that infusion through hollow microneedles into skin is limited by the resistance to flow offered by dense dermal tissue compressed during microneedle insertion.

MATERIALS AND METHODS

Microneedle Fabrication

Although microneedles can be mass-fabricated using a variety of different methods as single needles and multi-needle arrays made of a variety of different materials (23,24), we used single, glass microneedles in this study because they can be quickly produced in various geometries for small-scale laboratory use, are physiologically inert, permit easy visualization of fluid flow, and can be fabricated with dimensions similar to those of microfabricated microneedles. Glass microneedles were fabricated by pulling fire-polished borosilicate glass pipettes (o.d. 1.5 mm, i.d. 0.86 mm, BF150-86-15, Sutter Instrument, Novato, CA, USA) using a micropipette puller (P-97, Sutter Instrument). In most cases, the resulting blunt-tip microneedles were then beveled (BV-10, Sutter Instrument) and cleaned using chromic acid (Mallinckrodt, Hazelwood, MO, USA), followed by filtered DI water and acetone (J. T. Baker, Phillipsburg, NJ, USA) rinses. Microneedle geometries were determined by bright-field microscopy (Leica DC 300; Leica Microsystems, Bannockburn, IL, USA) and image analysis (Image Pro Plus, version 4.5, Media Cybernetics, Silver Spring, MD, USA). Microfabricated microneedles used in this study typically had an effective tip opening radius of 22–48 μm with a tip bevel angle of 35–38°. Because the opening of a bevel-tip microneedle is oval in shape, the effective radius was determined as the average of the half-lengths of the long and short axes of the ellipse.

Skin Preparation

Human abdominal skin was obtained from cadavers from the Emory University Body Donor Program and stored at −80°C (Revco Ultima II, Kendro Laboratory Products, Asheville, NC, USA). After warming to room temperature and removing subcutaneous fat, skin was hydrated in a Pyrex dish filled with phosphate-buffered saline (PBS; Sigma, St. Louis, MO, USA) for at least 15 min prior to use. The skin was then cut into 4 × 4 cm pieces and stretched onto a stainless-steel specimen board with eight tissue-mounting pins on it to mimic the tension of human skin *in vivo*.

Infusion Experiments

To measure flow rate into skin during microneedle infusion, a single microneedle was inserted into human cadaver skin to microinfuse sulforhodamine solution, and the infusion flow rate was measured over time. As an aid to visualizing flow into skin, sulforhodamine-B dye (Molecular Probes, Eugene, OR, USA) was added to PBS, stirred, and filtered (0.2-μm pore size, Nalge Nunc International, Rochester, NY, USA) to make 1×10^{-3} M sulforhodamine solution. Either a 250-μl or 1-ml glass syringe (Gastight Syringe, Hamilton Company, Reno, NV, USA) was used as the reservoir for sulforhodamine solution and was connected to a high-pressure CO_2 gas tank (Airgas, Radnor, PA, USA) on one end and connected to a 2.1-mm-i.d. metal tubing line on the other end, which was then connected to the end of a microneedle using a short, flexible tubing linker. A custom-made, rotary-threaded device (30) was used to hold the microneedle and to allow microneedle insertion into and retraction out of the skin in a controlled fashion calibrated by the number of rotations of the device (i.e., 1 full rotation = 1440-μm needle displacement). This assembly was held by a stainless-steel adapter attached to a Z-stage (Graduated Knob Unislide, Velmex, Bloomfield, NY, USA) to control vertical motion of the microneedle holder with ±10-μm resolution.

The flow rate of sulforhodamine solution microinjection was determined by following the movement of the gas–liquid meniscus in the syringe reservoir over time with a digital video camera (DCR-TRV460, Sony, Tokyo, Japan) and image

analysis software (Adobe Photoshop 7.0, Adobe Systems, San Jose, CA, USA) after converting the captured movie into sequences of still images (Adobe Premiere 6.0, Adobe Systems). After initially positioning the gas–liquid meniscus at the top of the glass syringe by injecting an appropriate amount of air upstream from the syringe, the microneedle was lowered until its tip touched the skin sample. The microneedle holder was then rotated clockwise to insert the microneedle to the desired insertion depth and sometimes rotated counterclockwise to retract the microneedle to the desired retraction distance.

The gas pressure was then set to the desired infusion pressure using a pressure regulator (Two-Stage Regulator, Fisher Scientific, Hampton, NH, USA) on the CO_2 cylinder and the experiment began. During the experiment, the skin was examined for fluid leakage, which was easily visible because of the presence of sulforhodamine dye in the fluid. If there was no leakage, then the flow rate within the glass syringe was assumed to be the same as the flow rate into the skin. This assumption was validated by preliminary experiments that quantified the sulforhodamine content of skin after microinjection using spectrofluorimetry after chemically digesting the skin. These measurements demonstrated that the amount of sulforhodamine within the skin was approximately the same as the amount displaced in the syringe source (data not shown). Data were discarded in those few cases (<5%) where leakage was observed.

To serve as a base case experiment, a bevel-tip microneedle with 30-μm effective opening radius was inserted to a depth of 1080 μm into the skin, and microinfusion flow was initiated by applying a constant infusion pressure of 138 kPa. Every 5 min, the needle was retracted 180 μm back toward the skin surface to a final insertion depth of 180 μm (relative to its initial position prior to insertion). The infusion flow rate was measured every minute with a 5-s offset at the beginning and the end of each period at a given retraction position (i.e., at 5, 60, 120, 180, 240, and 295 s).

To determine the effect of microneedle insertion depth and retraction distance on flow rate, the base case experiment was compared to otherwise identical experiments using 900- and 720-μm initial insertion depths followed by 180-μm retraction every 5 min. The effect of infusion pressure was determined by comparing to pressures of 69 and 172 kPa. The effect of tip bevel was determined by comparing to a blunt-tip microneedle with the same opening (i.e., 30-μm radius) as the bevel-tip microneedle. The effect of microneedle tip opening size was determined by comparing to needles with smaller (22-μm radius) and larger (48-μm radius) tip openings. The effect of hyaluronidase was determined by comparing to an infusion fluid containing 200 U/ml hyaluronidase prepared by mixing 3 ml of hyaluronidase solution (Vitrase®, 200 U/ml, ISTA Pharmaceuticals, Irvine, CA, USA) with 7 ml of 1×10^{-3} M sulforhodamine solution. Finally, the effect of infusion time was determined over longer times by inserting the microneedle to a depth of 1080 μm and either leaving it in place or retracting 720 μm to a final insertion depth of 360 μm and measuring flow rate for 104 min.

Histological and Microscopic Image Analysis

After each infusion experiment, the top surfaces and undersides of the skin were imaged using bright-field micros-

copy (Leica DC 300) to visualize the distribution of sulforhodamine infusion. Additional experiments were performed for detailed histological imaging of microneedle penetration pathways and injection within skin. For these experiments, a microneedle with 30-μm effective radius opening and 38° bevel angle was externally spray-coated (Testor Corporation, Rockford, IL, USA) using a solution of red dye (Tissue Marking Dye; Triangle Biomedical Sciences, Durham, NC, USA) thickened using 2×10^{-2} M polyvinylpyrrolidone (Aldrich, St. Louis, MO, USA). The needle was then inserted to a depth of 1080 μm into the skin and retracted 720 μm to a final insertion depth of 360 μm. A solution containing 2.1×10^8 particles/ml of 6-μm yellow-green fluorescence-labeled polystyrene microspheres (Fluoresbrite® YG, Polysciences, Warrington, PA, USA) mixed with blue-green dye (Triangle Biomedical Sciences) was injected at 138-kPa infusion pressure until the dye became visible within the skin (~1-min infusion time). These skin samples, with microneedles in place, were fixed using 10% neutral buffered formalin (Fisher Scientific) or a mixture of 2% paraformaldehyde and 2% glutaraldehyde (Electron Microscopy Sciences, Hatfield, PA, USA) for at least 24 h before rinsing thoroughly with PBS and then submerging in sterilized, filtered, 30% sucrose overnight (31). The skin samples were frozen in liquid nitrogen with optimal cutting temperature compound (Tissue-Tek, Sakura Finetek, Torrance, CA, USA) in an embedding mold container and later sectioned into 10-μm-thick slices using a cryostat (Cryo-star HM 560MV, Microm, Waldorf, Germany). Histological sections were surface-stained with hematoxylin and eosin (Autostainer XL, Leica Microsystems) and examined by bright-field (Leica DC 300) and fluorescence microscopy (Eclipse E600W, Nikon, Melville, NY, USA).

Statistical Analysis

Flow rate measurements at each condition and time point were performed using at least three skin specimens, from which the mean and standard deviation were calculated. A two-tailed Student's *t* test ($\alpha = 0.05$) was performed when comparing two experimental conditions. When comparing three or more experimental conditions, a one-way analysis of variance (ANOVA; $\alpha = 0.05$) was performed. A two-way analysis of variance ($\alpha = 0.05$) was performed when comparing two factors. In all cases, a value $p < 0.05$ was considered statistically significant.

RESULTS AND DISCUSSION

To determine the parameters controlling microinfusion into skin using microneedles, we flowed sulforhodamine solution into human cadaver skin and measured infusion flow rate as a function of microneedle insertion and retraction depths, infusion pressure, microneedle tip geometry, and presence of hyaluronidase. This study was motivated by the goal to identify methods that increase and control infusion into skin using microneedles. Analysis was guided by the hypothesis that infusion through hollow microneedles into skin is limited by the resistance to flow offered by dense dermal tissue compressed during microneedle insertion.

Fabrication and Characterization of Microneedles

Although clinical applications of microneedles are envisioned using multineedle arrays made of metal that are mass-produced by microfabrication, we used hand-drawn glass microneedles in this study to facilitate easy visualization of microinfusion into the skin and because of their versatility to be rapidly fabricated in various geometries. Although the micropipettes used in this study were much longer than microfabricated microneedles, the 1.1-mm or shorter portion of the micropipettes that protruded from the insertion device and inserted into the skin has dimensions very similar to microfabricated microneedles (i.e., width, taper, tip sharpness). We therefore expect that lessons learned with micropipettes used in the skin study are directly applicable to mass-produced microneedles. A representative glass microneedle is shown in Fig. 1. These needles could be repeatedly inserted into skin without breaking.

Single microneedles were inserted into human cadaver skin *in vitro* to a controlled depth and then, sometimes, partially retracted. Figure 2 shows a cross section of a piece of skin pierced with a microneedle and then chemically fixed for histological sectioning and staining. The hole made by the microneedle is evident, measuring 300–350 μm deep and having the same shape as the microneedle. Some deformation of the skin surface is also evident because of skin deflection during insertion. A small volume of dye was injected into the skin, and its infusion trajectory is also shown in Fig. 2. More dye is present on the right side of the image, presumably because the needle bevel was on the right and channeled flow in that direction. The directional nature of the flow further seems to be influenced by skin microstructure, where infusion pathways follow dermal collagen fiber orientation.

In a typical experiment, hundreds of microliters of fluid were infused into skin, which was distributed over an area measuring millimeters to centimeters across. Figure 3 shows representative images of the top and bottom surfaces of human cadaver skin after sulforhodamine infusion using a microneedle. All dye was contained within the skin and did not represent surface staining; leakage onto the skin surface during infusion was rarely seen. Dye distribution observed from the skin surface, shown as the circular dark area in Fig. 3A, was
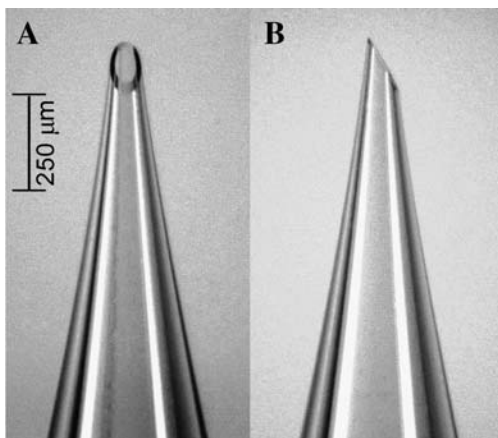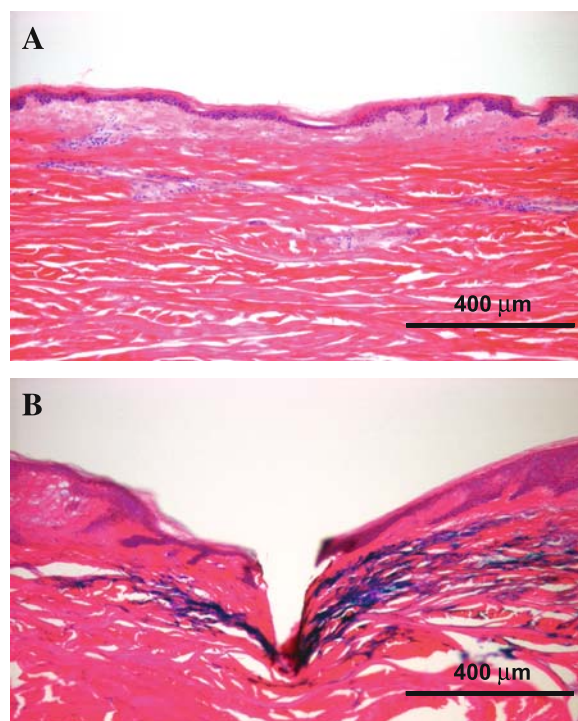

Fig. 2. Histological section of human cadaver skin (A) untreated and (B) pierced with a hollow microneedle *in vitro*. The needle was inserted to a depth of 1080 μm and then retracted 720 μm to a final insertion depth of 360 μm. The needle had a 36° beveled tip with a 32-μm effective radius opening. A small amount of blue dye was infused into the skin at a pressure of 138 kPa for 1 min, and then the skin was fixed with the needle in place. Before H&E staining and histological sectioning, the needle was removed and is not present in the image shown. The site of needle insertion is evident as the triangular region missing tissue, and the paths of fluid injection are indicated by the presence of blue dye.

generally more constrained than when viewed from underneath the skin, as shown by the widespread staining in Fig. 3B. Additional studies showed that microneedles could also be inserted into pig and rat cadaver skin to microinfuse sulforhodamine solution in a similar manner (data not shown).

Effect of Insertion and Retraction

To determine the effects of infusion parameters, microneedle infusion flow rates were measured over a range of different experimental conditions. Considering the most straightforward scenario of microneedle insertion without retraction, microneedle insertion to a depth of 1080 μm permitted sulforhodamine solution flow into the skin at a rate of 28 μl/h (Fig. 4A). Guided by our previous observations that subsequent needle retraction can increase flow rate (30), we partially retracted microneedles after insertion and found that retraction of the needle led to progressively larger flow rates, where a 900-μm retraction, corresponding to a net insertion of 180 μm, produced a flow rate of 326 μl/h. Initial insertion to lesser depths similarly produced low flow rates that were progressively increased with needle retraction (Fig. 4B and C). When these data from different insertion and retraction combinations are combined, a significant increase in flow rate with increasing retraction

Fig. 1. (A) Front and (B) side views of a representative hollow, glass microneedle. The microneedle shown has a tip opening effective radius of 30 μm in with a bevel angle of 38°.
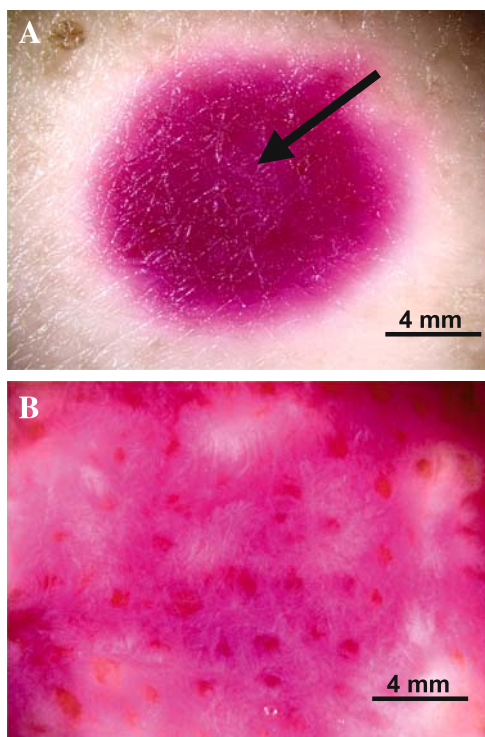
Fig. 3. (A) Top and (B) bottom surfaces of human cadaver skin after infusion of sulforhodamine solution using a hollow microneedle *in vitro*. Sites of sulforhodamine infusion are indicated by dark red staining. Infusion of 755 μl of solution was carried out over 104 min at 138 kPa using a microneedle with a 31-μm effective radius opening and a bevel angle of 37° inserted to a depth of 1080 μm into the skin and retracted 720 μm to a final insertion depth of 360 μm. The site of needle penetration is shown by the arrow in (A).

distance is apparent (Fig. 4D; ANOVA, $p < 0.05$). Further analysis also shows a significant increase in flow rate with increasing initial insertion depth (ANOVA, $p < 0.001$). Decreasing the net insertion depth, which corresponds to the initial insertion depth minus the retraction distance, also resulted in a larger flow rate (Fig. 4E; ANOVA, $p < 0.05$).

Considered together, these findings demonstrate that flow rate is largest when retraction distance is maximized by inserting deeply and retracting almost completely. This is consistent with our hypothesis that compressed dermal tissue blocks flow from microneedles because needle retraction should relieve compressive forces applied to the tissue by the microneedle and permit compressed dermal tissue to expand.

Effect of Infusion Pressure

Infusion pressure is expected to affect flow rate, and, as shown in Fig. 5, flow rate increased with increasing pressure (ANOVA, $p < 0.0001$). Increased infusion pressure certainly increased flow rate by increasing the pressure-driven driving force for flow, but might also act by displacing or deforming tissue to reduce resistance to flow. To decouple these two effects, we expect that flow rate should increase in direct proportion to pressure if pressure acts only as a driving force for convection [32]. In contrast, pressure-mediated changes in skin microstructure that reduce flow resistance are expected to have a nonlinear dependence on pressure [33, 34]. Guided by

these expected behaviors, the flow rate data shown in Fig. 5 were normalized by the infusion pressure. From 69 to 138 kPa, the increase in flow rate was proportional to the increase in pressure (ANOVA, $p = 0.14$). However, at 172 kPa, the flow rate showed a disproportionately large increase relative to the pressure increase (ANOVA, $p < 0.001$). This nonlinearity suggests that elevated pressure reduced flow resistance by displacing or deforming the dense dermal tissue impeding flow.

Effect of Microneedle Tip Bevel

Dermal tissue compressed by needle insertion should be most dense at the needle tip. Thus, flow from a blunt-tip microneedle, where the hole is located at the needle tip, should encounter greater resistance than flow from a bevel-tip microneedle, where the hole is off to the side. Consistent with this hypothesis, infusion flow rate from a bevel-tip microneedle was, on average, 3-fold greater than from a blunt-tip microneedle (Fig. 6; ANOVA, $p < 0.0001$).

Effect of Microneedle Tip Opening Size

If dense dermal tissue is the main barrier to flow, the size of the microneedle tip opening is expected to have only small effects because the microneedle itself does not impose the rate-limiting barrier. Consistent with this expectation, varying tip openings with effective radii ranging from 22 to 48 μm (i.e., areas ranging from 1462 to 7400 μm^2) had no significant effect on infusion flow rate (Fig. 7; ANOVA, $p = 0.27$). This suggests that the primary resistance to flow is not at the needle tip-to-skin interface, which would be heavily influenced by a 5-fold change in area. Instead, the volume of dense dermal tissue surrounding the tip seems to limit flow, where the size and density of this tissue is probably governed primarily by the depth of needle insertion and retraction, with little influence from tip opening size.

Effect of Hyaluronidase

Hyaluronidase is known to reduce flow resistance in the skin by rapidly breaking down hyaluronan, a glycosaminogly-can within skin collagen fibers (35–37). This enzyme might similarly break down the resistance of dermal tissue compressed during microneedle insertion. To test this prediction, microneedle infusion was carried out using our standard sulforhodamine solution mixed with a purified ovine testicular hyaluronidase preparation (Vitrase®) that is commercially available and FDA-approved for human use to facilitate injection when simultaneously coinjected using a hypodermic needle [38]. Addition of hyaluronidase increased infusion flow rate by 7-fold (Fig. 8; ANOVA, $p \leq 0.01$). This finding further supports the global hypothesis that dense dermal tissue limits flow from microneedles. It also suggests applications, where hyaluronidase or other compounds that affect skin microstructure could be coadministered to facilitate infusion using microneedles.

Microinfusion Over Time

In other scenarios, the resistance to fluid flow into tumor tissue at constant pressure has been shown to decrease over
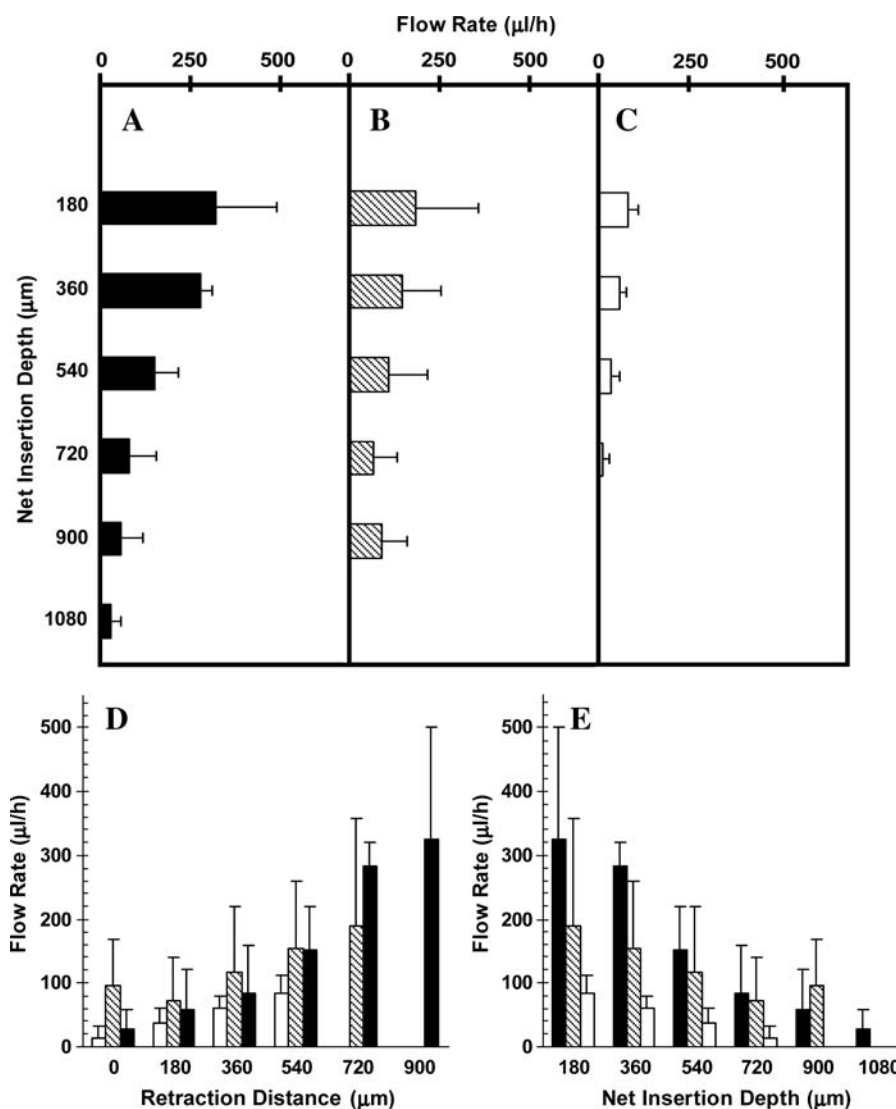
Fig. 4. Effect of insertion depth and retraction distance on flow rate into human cadaver skin *in vitro*. Microneedles were initially inserted to a maximum insertion depth of (A) 1080 μm, (B) 900 μm, or (C) 720 μm and then retracted various distances back toward the skin surface to a final, net insertion depth. Pooling the data from parts (A), (B), and (C), flow rate is shown as a function of (D) retraction distance and (E) net insertion depth for maximum insertion depths of 720 μm (white bars), 900 μm (striped bars), and 1080 μm (black bars). Microneedles had tip opening effective radii of 27–31 μm with bevel angles of 35–37°. Infusion was performed for 5 min at 138 kPa without needle retraction, after which, microneedles were retracted by 180 μm every 5 min to a final insertion depth of 180 μm. Data are expressed as mean values ($n \geq 3$) with standard deviation bars.

time, probably because of flow-induced changes in tissue microstructure (33,34). To address this possibility during infusion using microneedles, we measured flow into skin continuously for 100 min for needles inserted and left in place and for needles inserted and retracted (Fig. 9). In both cases, the cumulative volume of fluid infused into skin increased linearly with time (linear regression correlation coefficient, $R^2 > 0.99$), suggesting that skin resistance to flow did not change over the timescale studied. Note that the pressure used in this experiment was less than the pressure identified previously to induce nonlinear changes in flow rate (Fig. 5), which is consistent with this observation that flow rate did not change with time. Despite the generally

linear trend, the flow rate was transiently higher at the onset of flow and then decayed within a few minutes to a steady state (Fig. 9, inset). This effect might be explained by the rapid filling of a small cavity in the skin at the needle tip formed by the insertion/retraction process, followed by slower infusion into and across intact, compressed tissue.

Tissue Resistance is Significantly Higher than that Offered by Microneedles

Tissue resistance is expected to be the dominant resistance to flow when compared to the resistance offered by the microneedle itself during a microneedle injection into
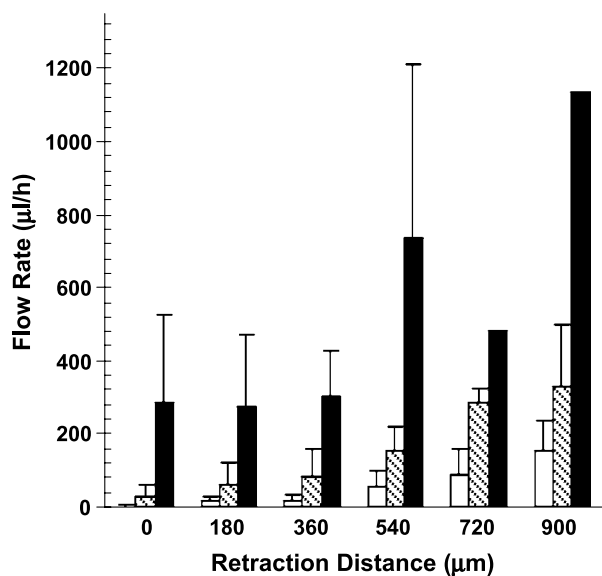
Fig. 5. Effect of pressure on flow rate into human cadaver skin. Microinfusion flow rate was measured as a function of retraction distance at three pressures: 69 kPa (white bars), 138 kPa (striped bars), and 172 kPa (black bars). Microneedles having 35–37° beveled tips with 27- to 32-μm effective radius openings were inserted to a maximum depth of 1080 μm. Data are expressed as mean values ($n \geq 3$) with standard deviation bars.

skin. To test this hypothesis, flow rate measurements from a previous study (39), which corresponds to flow of fluid through microneedles into the air (i.e., without the presence of skin), was plotted together with a subset of flow rate measurements in Figs. 5 and 8, which correspond to flow of fluid through microneedles during microinfusion into skin (i.e., at infusion pressures of 69, 138, and 172 kPa with and
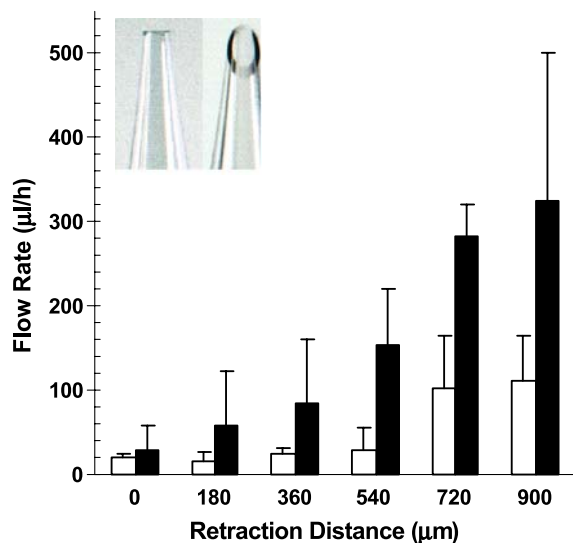

Fig. 7. Effect of tip opening size on flow rate into human cadaver skin. Microinfusion flow rate was measured as a function of retraction distance using three different tip opening sizes: 22 μm (black bars; left inset image), 30 μm (striped bars; center inset image), and 48 μm (white bars; right inset image) effective radii. Microneedles having 35–37° beveled tips were inserted to a maximum depth of 1080 μm, and infusion was carried out at 138 kPa. Data are expressed as mean values ($n \geq 3$) with standard deviation bars.
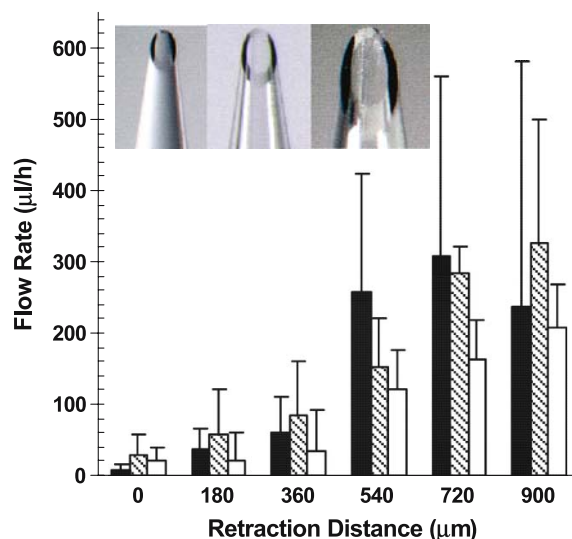
without the presence of hyaluronidase). This comparison is shown in Fig. 10, which indicates that the presence of skin tissue decreases the flow rate by as much as a few orders of magnitude. Overall, this result suggests that dermal tissue offers significant resistance to flow during microinfusion using microneedles into skin.
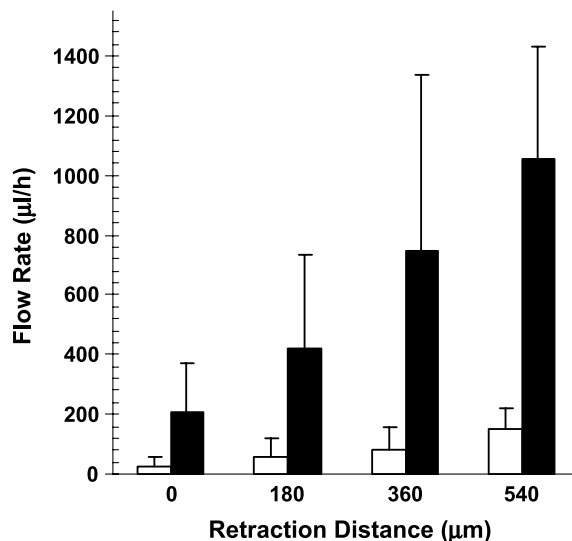

Fig. 6. Effect of tip bevel on flow rate into human cadaver skin. Microinfusion flow rate was measured as a function of retraction distance during infusion using hollow microneedles with a blunt tip (white bars; left inset image) and a 35° beveled tip (black bars; right inset image). Microneedles with 27- to 32-μm effective radius openings were inserted to a maximum depth of 1080 μm, and infusion was carried out at 138 kPa. Data are expressed as mean values ($n \geq 3$) with standard deviation bars.

Fig. 8. Effect of hyaluronidase on flow rate into human cadaver skin. Microinfusion flow rate was measured as a function of retraction distance during infusion in the absence (white bars) or presence (black bars) of hyaluronidase. Microneedles having 35–37° beveled tips with 27- to 32-μm effective radius openings were inserted to a maximum depth of 1080 μm, and infusion was carried out at 138 kPa. Data are expressed as mean values ($n \geq 3$) with standard deviation bars.

Implications for Drug Delivery Applications

This study shows that microneedles can infuse fluid into skin over a range of flow rates that can be controlled by infusion parameters. Flow rate was maximized by infusing at high pressure with hyaluronidase through beveled needles inserted deeply and retracted almost completely. These effects can be explained by the overall hypothesis that infusion through hollow microneedles into skin is limited by the resistance to flow offered by dense dermal tissue compressed during microneedle insertion. Needle retraction increases flow rate by relieving compressive forces applied to the tissue by the microneedle and allowing compressed tissue to expand. Increased pressure also increases flow rate by increasing the driving force and by displacing or deforming tissue to reduce resistance to flow. A beveled microneedle reduces flow resistance by infusing to the side of the dense tissue formed at the needle tip. Hyaluronidase attacks extracellular matrix structures within skin to rapidly break down the barriers to flow. Needle tip opening size did not affect infusion because the compression of tissue at the needle tip is governed primarily by the depth of needle insertion and retraction.

This study is significant because it is the first to systematically examine the effects of infusion parameters and optimize them to increase flow rate into skin using hollow microneedles. In contrast to previous microneedle studies that infused relatively small volumes using nonoptimized protocols, this study provides strategies to increase flow rate using appropriate insertion protocols and needle design. In addition to these experimental observations, the mechanistic interpretation that compressed tissue is a rate-limiting barrier to flow provides a rational approach to further optimize infusion methods and design new approaches.
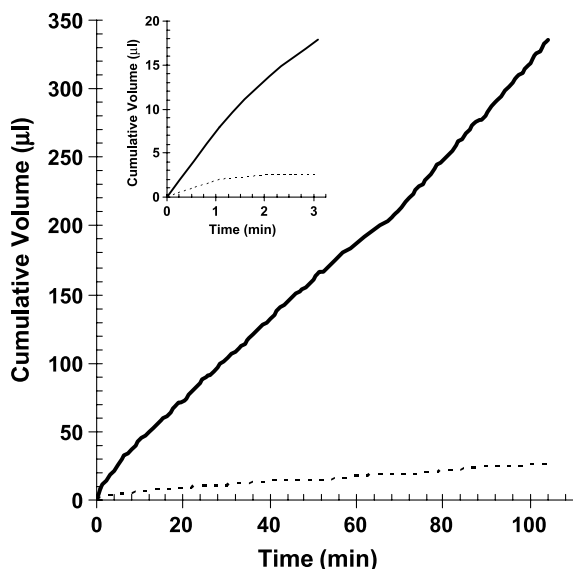

Fig. 9. Cumulative infusion volume during infusion into human cadaver skin over time for microneedles inserted into skin to a depth of 1080 μm and then retracted 720 μm to a final insertion depth of 360 μm (solid line) and microneedles inserted to a depth of 1080 μm without retraction (dashed line). Infusion was carried out at 138 kPa using microneedles having 35–38° beveled tips with 30–32 μm effective radius openings. Data are expressed as mean values ($n \geq 3$) with average standard deviation of 40% for both curves (not shown).
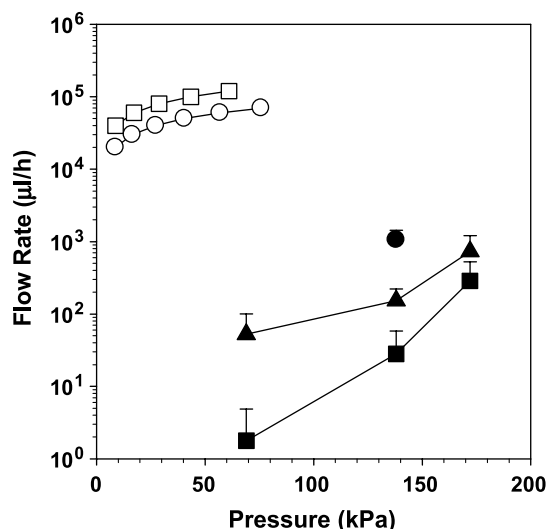

Fig. 10. Effect of skin on flow rate through microneedles. Fluid flow rate was measured as a function of pressure across microneedles with (black symbols) and without (white symbols) the presence of skin. Fluid flow rates through microneedles with (○) 25-μm and (□) 34-μm radii [data from (40)] were compared to those with the skin present, in which microinfusion into skin using microneedles was performed with insertion depth of 1080 μm without retraction (■), with insertion depth of 1080 μm and retracted 540 μm without the presence of hyaluronidase (▲), and with the presence of hyaluronidase (●) (data from Figs. 5 and 8). Data are expressed as mean values ($n \geq 3$) with standard deviation bars.

Single microneedles were shown to infuse fluid into skin at flow rates up to 1 ml/h, which is sufficient for many applications. Delivery from an array containing multiple needles should increase flow rates further, possibly increasing linearly with the number of needles. In this way, hollow microneedles can be envisioned as a minimally invasive alternative to conventional infusion sets based on hypodermic needles and catheters. In one scenario, microneedles could be coupled with a commercially available infusion pump to provide a patient-friendly needle alternative that could be especially attractive for home use by patients. Because of their low profile, microneedles could also be mounted on the base of a small, "wearable" pump that could be applied to the skin much like an oversized patch for still greater patient convenience. Potential applications of this technology include insulin, hormonal therapies requiring pulsatile delivery, and drugs with short half-lives that require frequent administration.

Despite these opportunities, there are limitations to infusion using microneedles. The maximum flow rate observed in this study is much slower than hypodermic injection, suggesting that microneedles are not appropriate when rapid bolus delivery is needed, e.g., in emergency situations. Moreover, some infusion protocols require intravenous administration, which microneedles cannot achieve, inherent to their design. Although average flow rate over extended time was stable for 100 min in this study, instantaneous flow rate showed some instability using a constant pressure driving force (e.g., Fig. 9). This problem could be addressed by using a constant flow rate pump instead. Finally, cost-effective applications will require replacing the single, hand-drawn, glass needles used in this study with arrays of metal microneedles mass-produced by adapting existing microfabrication technology and integrating

them into user-friendly devices containing a drug reservoir, micropump, and microelectronic controls.

CONCLUSIONS

Guided by the hypothesis that infusion through hollow microneedles into skin is limited by the resistance to flow offered by dense dermal tissue compressed during micro-needle insertion, this study systematically examined the effects of infusion parameters and optimized them to increase flow rate into skin. Overall, flow rate was optimized by inserting needles deeply and then retracting almost completely, infusing at high pressure, using microneedles with a beveled tip, and adding hyaluronidase to the infusion fluid. Microneedle tip opening size did not significantly affect flow rate. Infusion over longer times demonstrated a constant flow rate after a short, transient burst at constant pressure. Altogether, this study shows that hollow microneedles can be designed to infuse milliliter quantities of fluid into skin to make transdermal delivery of many drugs possible and to provide a minimally invasive alternative to conventional infusion sets based on hypodermic needles and catheters.

ACKNOWLEDGMENTS

REFERENCES

1. I. Findley and G. Chamberlain. ABC of labour care: relief of pain. *Br. Med. J.* **318**:927–930 (1999).
2. A. J. Fox and D. J. Rowbotham. Recent advances: anaesthesia. *Br. Med. J.* **319**:557–560 (1999).
3. C. Pasero. Subcutaneous opioid infusion. *Am. J. Nurs.* **102**:61–62 (2002).
4. B. W. Bode, H. T. Sabbah, T. M. Gross, L. P. Fredrickson, and P. C. Davidson. Diabetes management in the new millennium using insulin pump therapy. *Diabetes/Metab. Res. Rev.* **18**:S14–S20 (2002).
5. M. J. Lenhard and G. D. Reeves. Continuous subcutaneous insulin infusion: a comprehensive review of insulin pump therapy. *Arch. Intern. Med.* **161**:2293–2300 (2001).
6. J. L. Colquitt, C. Green, M. K. Sidhu, D. Hartwell, and N. Waugh. Clinical and cost-effectiveness of continuous subcutaneous insulin infusion for diabetes. *Health Technol. Assess.* **8**:1–202 (2004).
7. A. Liebl. Challenges in optimal metabolic control of diabetes. *Diabetes/Metab. Res. Rev.* **18**:S36–S41 (2002).
8. D. E. Moulin and J. H. Kreeft. Comparison of continuous subcutaneous and intravenous hydromorphone infusions for management of cancer pain. *Lancet* **337**:465–468 (1991).
9. E. Meehan, Y. Gross, D. Davidson, M. Martin, and I. Tsals. A microinfusor device for the delivery of therapeutic levels of peptides and macromolecules. *J. Control. Release* **46**:107–116 (1997).
10. P. M. Lynch, J. Butler, D. Huerta, I. Tsals, D. Davidson, and S. Hamm. A pharmacokinetic and tolerability evaluation of two continuous subcutaneous infusion systems compared to an oral controlled-release morphine. *J. Pain Symptom Manage.* **19**:348–356 (2000).
11. R. Jolanki, L. Kanerva, T. Estlander, M.-L. Henriks-Eckerman, and R. Suhonen. Allergic contact dermatitis from phenoxyethoxy ethylacrylates in optical fiber coating, and glue in an insulin pump set. *Contact Dermatitis* **45**:36–37 (2001).
12. S. Henry, D. V. McAllister, M. G. Allen, and M. R. Prausnitz. Microfabricated microneedles: a novel approach to transdermal drug delivery. *J. Pharm. Sci.* **87**:922–925 (1998).
13. D. V. McAllister, P. M. Wang, S. P. Davis, J.-H. Park, P. J. Canatella, M. G. Allen, and M. R. Prausnitz. Microfabricated needles for transdermal delivery of macromolecules and nanoparticles: fabrication methods and transport studies. *Proc. Natl. Acad. Sci. USA* **100**:13755–13760 (2003).
14. F. Chabri, K. Bouris, T. Jones, D. Barrow, A. Hann, C. Allender, K. Brain, and J. Birchall. Microfabricated silicon microneedles for nonviral cutaneous gene delivery. *Br. J. Dermatol.* **150**:869–877 (2004).
15. W. Martanto, S. P. Davis, N. R. Holiday, J. Wang, H. S. Gill, and M. R. Prausnitz. Transdermal delivery of insulin using micro-needles *in vivo*. *Pharm. Res.* **21**:947–952 (2004).
16. W. Lin, M. Cormier, A. Samiee, A. Griffin, B. Johnson, C. L. Teng, G. E. Hardee, and P. E. Daddona. Transdermal delivery of antisense oligonucleotides with microprojection patch (Macroflux) technology. *Pharm. Res.* **18**:1789–1793 (2001).
17. M. Cormier and P. E. Daddona. Macroflux technology for transdermal delivery of therapeutic proteins and vaccines. In M. J. Rathbone, J. Hadgraft, and M. S. Roberts (eds.), *Modified-Release Drug Delivery Technology*, Marcel Dekker, New York, NY, 2003, pp. 589–598.
18. M. Cormier, B. Johnson, M. Ameri, K. Nyam, L. Libiran, D. D. Zhang, and P. Daddona. Transdermal delivery of desmopressin using a coated microneedle array patch system. *J. Control. Release* **97**:503–511 (2004).
19. J. A. Matriano, M. Cormier, J. Johnson, W. A. Young, M. Buttery, K. Nyam, and P. E. Daddona. Macroflux microprojection array patch technology: a new and efficient approach for intracutaneous immunization. *Pharm. Res.* **19**:63–70 (2002).
20. J. A. Mikszta, J. B. Alarcon, J. M. Brittingham, D. E. Sutter, R. J. Pettis, and N. G. Harvey. Improved genetic immunization via micromechanical disruption of skin-barrier function and targeted epidermal delivery. *Nat. Med.* **8**:415–419 (2002).
21. J. A. Mikszta, V. J. Sullivan, C. Dean, A. M. Waterston, J. B. Alarcon, J. P. Dekker, III, J. M. Brittingham, J. Huang, C. R. Hwang, M. Ferriter, G. Jiang, K. Mar, K. U. Saikh, B. G. Stiles, C. J. Roy, R. G. Ulrich, and N. G. Harvey. Protective immunization against inhalational anthrax: a comparison of minimally invasive delivery platforms. *J. Infect. Dis.* **191**:278–288 (2005).
22. S. Kaushik, A. H. Hord, D. D. Denson, D. V. McAllister, S. Smitra, M. G. Allen, and M. R. Prausnitz. Lack of pain associated with microfabricated microneedles. *Anesth. Analg.* **92**:502–504 (2001).
23. D. V. McAllister, M. G. Allen, and M. R. Prausnitz. Microfabricated microneedles for gene and drug delivery. *Annu. Rev. Biomed. Eng.* **2**:289–313 (2000).
24. M. L. Reed and W.-K. Lye. Microsystems for drug and gene delivery. *Proc. IEEE* **92**:56–75 (2004).
25. H. J. G. E. Gardeniers, R. Luttge, E. J. W. Berenschot, M. J. de Boer, S. Y. Yeshurun, M. Hefetz, R. van't Oever, and A. van den Berg. Silicon micromachined hollow microneedles for transdermal liquid transport. *J. MEMS* **12**:855–862 (2003).
26. J. Chen, K. D. Wise, J. F. Hetke, and S. C. Bledsoe Jr. A multichannel neural probe for selective chemical delivery at the cellular level. *IEEE Trans. Biomed. Eng.* **44**:760–769 (1997).
27. B. Stoeber and D. Liepmann. *Design, fabrication, and testing of a MEMS Syringe, Proceedings of Solid-State Sensor and Actuator Workshop*, Transducers Research Foundation, Hilton Head Island, SC, USA, 2002.
28. S. P. Davis, W. Martanto, M. G. Allen, and M. R. Prausnitz. Hollow metal microneedles for insulin delivery to diabetic rats. *IEEE Trans. Biomed. Eng.* **52**:909–915 (2005).
29. W. H. Smart and K. Subramanian. The use of silicon micro-fabrication technology in painless blood glucose monitoring. *Diabetes Technol. Ther.* **2**:549–559 (2000).
30. P. M. Wang, M. Cornwell, J. Hill, and M. R. Prausnitz. Precise microinjection into skin using hollow microneedles. (submitted)
31. P. M. Wang, M. Cornwell, and M. R. Prausnitz. Minimally invasive extraction of dermal interstitial fluid for glucose

monitoring using microneedles. *Diabetes Technol. Ther.* **7**:131–141 (2005).

32. J. D. Bancroft and M. Gamble. *Theory and Practice of Histological Techniques*, Churchill Livingstone, New York, NY, 2002.
33. R. W. Fox and A. T. McDonald. *Introduction to Fluid Mechanics*, Wiley, New York, NY, 1998.
34. X.-Y. Zhang, J. Luck, M. W. Dewhirst, and F. Yuan. Interstitial hydraulic conductivity in a fibrosarcoma. *Am. J. Physiol. Heart Circ. Physiol.* **279**:H2726–H2734 (2000).
35. S. McGuire and F. Yuan. Quantitative analysis of intratumoral infusion of color molecules. *Am. J. Physiol. Heart Circ. Physiol.* **281**:H715–H721 (2001).
36. G. Kreil. Hyaluronidases—a group of neglected enzymes. *Protein Sci.* **4**:1666–1669 (1995).
37. E. Bruera, C. M. Neumann, E. Pituskin, K. Calder, and J. Hanson. A randomized controlled trial of local injections of hyaluronidase versus placebo in cancer patients receiving subcutaneous hydration. *Ann. Oncol.* **10**:1255–1258 (1999).
38. K. Meyer. Hyaluronidases. In P. D. Boyer (ed.), *The Enzymes,* Vol. 5, Academic Press, New York, NY, 1971, pp. 307–320.
39. Hyaluronidase (Vitrase)-ISTA. *Drugs R&D* **4**:194–197 (2003).
40. W. Martanto, M. K. Smith, S. M. Baisch, E. A. Costner, and M. R. Prausnitz. Fluid dynamics in conically tapered microneedles. *AIChE J.* **51**:1599–1607 (2005).